Journal of Medicinal Chemistry

Article

pubs.acs.org/jmc

Discovery of Competitive and Noncompetitive Ligands of the Organic Cation Transporter 1 (OCT1; SLC22A1)

Eugene C. Chen,[†,#,○] Natalia Khuri,[†,∇,○] Xiaomin Liang,[†,○] Adrian Stecula,[†] Huan-Chieh Chien,[†] Sook Wah Yee,[†] Yong Huang,[‡] Andrej Sali,[†,§,∥] and Kathleen M. Giacomini*[,†,§,∥,⊥]

[†]Department of Bioengineering and Therapeutic Sciences, University of California, San Francisco, California 94143, United States
[‡]Optivia Biotechnology, Menlo Park, California 94025, United States
[§]Department of Pharmaceutical Chemistry, University of California, San Francisco, California 94158, United States
[∥]California Institute of Quantitative Biosciences, University of California, San Francisco, California 94158, United States
[⊥]Institute of Human Genetics, University of California, San Francisco, California 94143, United States

Supporting Information

ABSTRACT: Organic cation transporter 1 (OCT1) plays a critical role in the hepatocellular uptake of structurally diverse endogenous compounds and xenobiotics. Here we identified competitive and noncompetitive OCT1-interacting ligands in a library of 1780 prescription drugs by combining in silico and in vitro methods. Ligands were predicted by docking against a comparative model based on a eukaryotic homologue. In parallel, high-throughput screening (HTS) was conducted using the fluorescent probe substrate ASP^+ in cells overexpressing human OCT1. Thirty competitive OCT1 ligands, defined as ligands predicted in silico as well as found by HTS, were identified. Of the 167 ligands identified by HTS, five were predicted to potentially cause clinical drug interactions. Finally, virtual screening of 29 332 metabolites predicted 146 competitive OCT1 ligands, of which an endogenous neurotoxin, 1-benzyl-1,2,3,4-tetrahydroisoquinoline, was experimentally validated. In conclusion, by combining docking and in vitro HTS, competitive and noncompetitive ligands of OCT1 can be predicted.

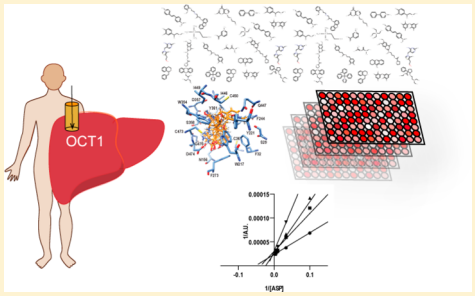

INTRODUCTION

Organic cation transporter 1 (OCT1; SLC22A1), a polyspecific membrane transporter, is among the most abundantly expressed transporters in human liver. Localized to the sinusoidal membrane of hepatocytes, OCT1 mediates the hepatic uptake of a diverse array of small positively charged hydrophilic compounds, including many endogenous bioactive amines[1] (e.g., dopamine, histamine, and serotonin). We recently identified OCT1 as a high-capacity transporter of thiamine in the liver and showed that the transporter plays a key role in modulating hepatic energy status and lipid content.[2]

Although the transporter clearly has important endogenous functions,[2,3] OCT1 has been characterized primarily as a drug transporter, capable of transporting a wide variety of prescription drugs, including the antidiabetic drug metformin and the opioid analgesic morphine. Genetic variants of OCT1 with reduced function have been associated with decreased response to metformin[4] as well as high systemic plasma levels of morphine and the active metabolite of the opioidergic drug tramadol.[5] Furthermore, administration of the calcium channel blocker verapamil (a potent inhibitor of OCT1) has been shown to reduce response to metformin, presumably through reducing hepatic drug levels.[6] In recognition of its critical role in drug disposition and response, OCT1 was included in a group of transporters of clinical importance by the International Transporter Consortium.[7] In 2012, the European Medicines Agency (EMA) recommended in vitro inhibition studies against OCT1 for investigational drugs in its Guidance on the Investigation of Drug Interactions.[8]

To date, more than 50 inhibitors of OCT1 transport have been identified by in vitro inhibition studies using radioactive or fluorescent probe substrates.[9,10] However, these studies have not identified the mechanisms by which inhibitors modulate OCT1 transport. Growing evidence suggests that OCT1-mediated transport can be inhibited in a "substrate-dependent" manner due to the presence of multiple, possibly overlapping binding sites on the protein.[11] Identification and characterization of OCT1 ligands could be facilitated by the availability of an atomic structure. However, the three-dimensional (3D) structures of human OCT1 and its mammalian orthologues have not yet been determined. Although several residues important for substrate binding have been reported and rationalized with OCT1 comparative models built using atomic structures of bacterial homologues,[12−17] accurate prediction of the binding site(s) remains challenging because of the low sequence identity between bacterial proteins and human OCT1. Recently, a structure of a high-affinity phosphate

Received: September 1, 2016
Published: February 23, 2017

DOI: 10.1021/acs.jmedchem.6b01317
J. Med. Chem. 2017, 60, 2685−2696

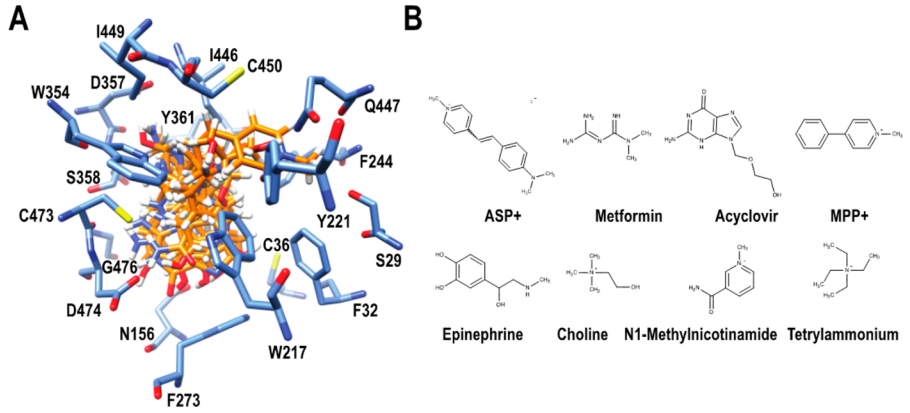

Figure 1. Predicted binding site of OCT1 and representative substrates. (A) Thirteen residues (S29, F32, C36, N156, Y221, F273, W354, Y361, I446, S358, C450, C473, and D474) formed hydrogen bonds with docked substrate molecules. Six residues in the predicted binding site (W217, F244, I449, D357, Q447, and G476) participated in non-covalent and/or polar substrate−transporter interactions. OCT1 residues are shown as cornflower blue sticks. Structures of 12 favorably docked known OCT1 substrates are shown as orange sticks. Oxygen, nitrogen, sulfur, and hydrogen atoms are depicted in red, dark blue, yellow, and white, respectively. (B) 2D structures of representative OCT1 substrates drawn using MarvinView 14.7.7.0 (ChemAxon).

transporter from the fungus *Piriformospora indica* (PiPT) was determined by X-ray crystallography.[18] The transporter shares approximately 20% sequence identity with human solute carrier (SLC) transporters, especially within the SLC22 family, thus providing a new opportunity for comparative modeling of OCT1 and virtual screening.[18]

We used a combination of in silico and high-throughput screening (HTS) methods to identify prescription drugs and endogenous metabolites that are ligands of OCT1, with the goals of predicting clinical drug interactions and understanding their interactions with OCT1 protein. To this end, we screened a prescription drug library in silico for compounds that interact with a predicted binding site on OCT1 using comparative structure modeling and virtual docking. In parallel, we conducted HTS for inhibitors of OCT1-mediated transport of the fluorescent ligand ASP^+ against the same prescription drug library. We identified 167 ligands in the screened library and predicted 30 competitive ligands. Moreover, we showed that combining structure-guided ligand discovery with structure−activity relationship models from HTS data enables the prediction of competitive ligands of OCT1 from endogenous and exogenous metabolites.

RESULTS

Comparative Model of OCT1 and Its Validation by Docking of Known Substrates. We modeled human OCT1 on the basis of the 2.9 Å structure of PiPT, a high-affinity phosphate transporter from *Piriformospora indica*, crystallized in an inward-facing occluded state with a bound substrate[18] (Protein Data Bank ID 4J05). The best-scoring 3D model was selected using the normalized discrete optimized protein energy (zDOPE) potential.[19] The zDOPE score of −0.22 suggests that 60% of its Cα atoms are within 3.5 Å of their correct positions.[20] The model includes all 12 transmembrane helices (TMHs), organized into the N- and C-terminal domains, and putative binding sites were identified in the translocation cavity between the two domains.[13] The following regions were not modeled: a large extracellular loop between TMHs 1 and 2, an intracellular loop between TMHs 6 and 7, and the intracellular N- and C-termini. While these regions may play a role in OCT1 homo-oligomerization, studies in rat showed that homo-oligomerization does not affect substrate affinity and transport function.[21] Because ASP^+ was used as a probe substrate, we first docked ASP^+ into two predicted binding sites and selected the site with the best score (−6.08) for all subsequent docking. Next, we validated the accuracy of the comparative model of the OCT1 transporter by confirming that (1) known OCT1 substrates docked favorably against the predicted binding site and (2) residues implicated in OCT1 transport[12,14,16,17] were localized in the predicted binding site, as follows. First, we docked 15 known OCT1 endogenous and drug substrates against the predicted binding site (Figure 1A). Twelve out of 15 substrates (80%) had favorable (negative) docking scores, ranging from −24.44 for acyclovir to −2.88 for oxaliplatin (Figure 1B and Table S1). The positive scores for three compounds (e.g., prostaglandins and pentamidine) resulted from steric clashes between ligand and transporter atoms, indicating that either the predicted binding site is too small to accommodate larger OCT1 ligands or that these compounds bind at a different site in the translocation pore. We also performed an enrichment analysis of docked substrates and decoys and computed a logAUC metric of 22.94, which suggests docking accuracy comparable to that in previously reported virtual screening experiments for human SLC transporters.[22,23] Second, we analyzed favorable docking poses to determine the frequency of predicted hydrogen bonds between binding site residues and substrate molecules. Thirteen residues in TMHs 4, 10, and 11 formed hydrogen bonds with substrate molecules (Figure 1A). Previous mutagenesis studies and homology modeling efforts suggested that these residues are important for substrate binding and OCT1-mediated transport in other species.[12−17] In particular, negatively charged D474 is important for interactions with positively charged OCT1 substrates. Additionally, in rat, mutations of Y221 and D474 resulted in reduced uptake of tetraethylammonium (TEA).[16] Finally, docked substrates formed non-covalent interactions with W217, T225, I449, and Q447 in TMHs 4, 10, and 11. The equivalent residues in rat have also been implicated in ligand−transporter interactions.[17]

Prediction of New Ligands by Virtual Screening and Validation by HTS. We predicted new ligands of OCT1 by docking each one of the 1780 compounds in the Pharmakon drug library (MicroSource Discovery Systems; http://www.

DOI: 10.1021/acs.jmedchem.6b01317
J. Med. Chem. 2017, 60, 2685−2696

msdiscovery.com/) against the predicted binding site on the OCT1 model. From the 1780 compounds, 471 putative OCT1 ligands were predicted (normalized docking scores less than −1). These predictions were then tested by HTS of the entire Pharmakon library. The HTS assay relied on the uptake of the fluorescent substrate ASP^+ by OCT1-overexpressing HEK cells to assess the activity of the transporter.[10,24] The uptake of ASP^+ was linear for the first 5 min, and the K_m was determined to be 21.2 μM (Figure 2A,B). Thus, a substrate concentration of 2

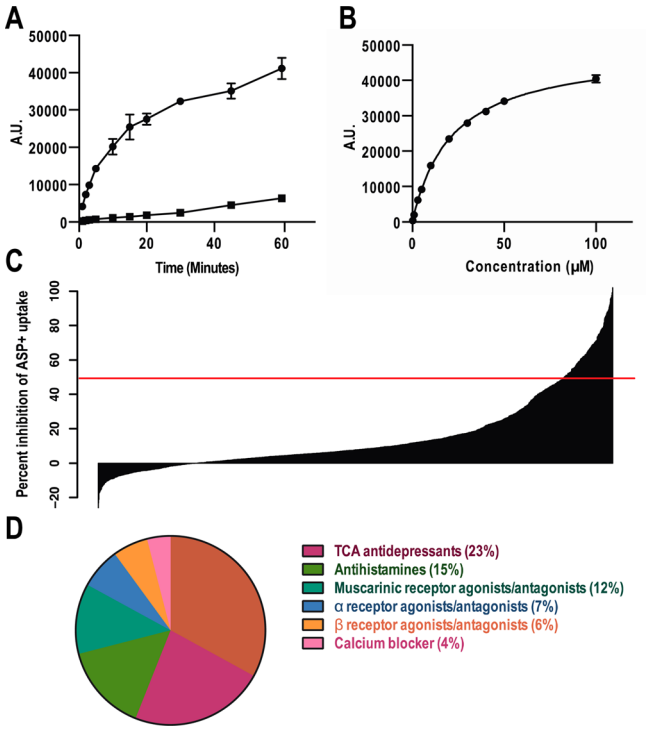

Figure 2. Uptake of ASP^+ and HTS screening data. (A) Time-dependent ASP^+ uptake in HEK cells overexpressing OCT1 (●) or empty vector (■). (B) Overexpression of OCT1 increases ASP^+ uptake in HEK cells. ASP^+ uptake studies were conducted in HEK cells overexpressing OCT1 or empty vector. Cells were incubated with increasing concentrations of ASP^+ for 2 min. The uptake kinetic parameters were calculated using the difference in ASP^+ accumulation between cells overexpressing OCT1 and empty vector cells. Each data point represents mean ± SD, n = 6. (C) Distribution of inhibition values from HTS of 1780 compounds. A total of 167 inhibitors were identified among the 1780 Pharmakon compounds. (D) Distribution of the 167 inhibitors in various pharmacological classes. Brown color represents mixed class.

μM was used to minimize the effect of substrate concentration on the IC_{50} values, and an incubation time of 2 min was used to measure the initial rate of uptake. The average Z-prime score of the HTS was 0.80, indicating a reproducible assay.[25] Of the 1780 Pharmakon compounds, 167 compounds (9%) were determined to be OCT1 inhibitors (Figure 2C), defined as compounds that inhibited 50% or more of ASP^+ uptake at 20 μM. Drugs known to inhibit OCT1 activity at 20 μM were generally confirmed by the screen. Of the 167 compounds, 30 were also predicted as ligands by virtual screening. The overall accuracy of virtual screening was 70%. The sensitivity and specificity of predictions were 77% and 12%, respectively. The low specificity is not surprising because the docking pipeline was executed in a fully automated fashion; in contrast, typical structure-based virtual screening involves manual postdocking selection of ligand poses.[22,23,26]

We examined compounds predicted to be OCT1 ligands by the comparative model but not identified as inhibitors by HTS. In view of the published literature, we identified 13 previously reported substrates and five inhibitors of OCT1. Among these predicted ligands, cimetidine (rank #21), metformin (rank #84), and thiamine (rank #200) inhibited OCT1-mediated uptake of ASP^+ by 4.13%, 11.1%, and −1.5%, respectively. The docking poses of all three compounds predicted favorable interactions with the comparative model; in particular, metformin and cimetidine formed hydrogen bonds with Asp474 (Figure 3A,B). The inability of HTS to identify some

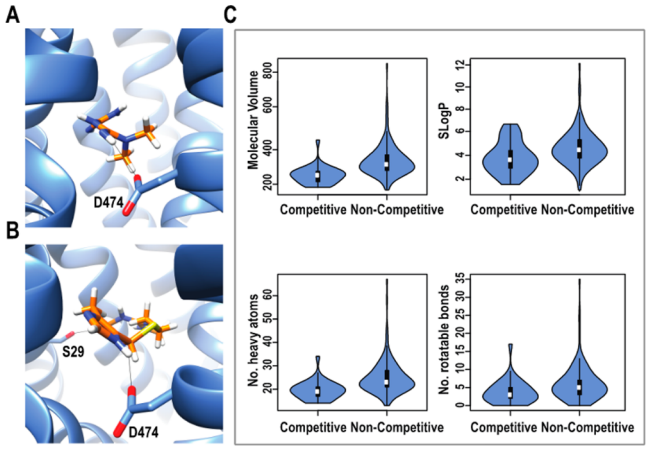

Figure 3. Docking results and physiochemical properties of OCT1 ligands in the Pharmakon library. Compounds are shown in orange sticks and hydrogen bonds as black dotted lines. (A) Predicted pose of metformin and its hydrogen bond with aspartic acid residue 474. (B) Predicted pose of cimetidine and its hydrogen bonds with D474 and S29. (C) Differences in distribution of physicochemical properties for predicted competitive (n = 30) and noncompetitive (n = 137) inhibitors of OCT1. Only significantly different distributions are shown (Student's t test, $p < 0.05$).

of the previously reported ligands can be explained by their OCT1 affinity, which is much weaker than that of ASP^+. For example, the reported IC_{50} values of cimetidine and metformin for inhibition of OCT1-mediated transport of YM155 and MPP^+ were 149 and 1230 μM, respectively,[27,28] and the IC_{50} of thiamine was determined to be 4.1 mM (Figure S1). Because our HTS assay measured inhibition of OCT1 activity by test compounds at 20 μM, it was unable to identify ligands such as cimetidine, metformin, and thiamine.

HTS identified tricyclic antidepressants, antihistamines, and α-adrenergic receptor agonists, agreeing with previously published results.[10] HTS also identified a high proportion of ligands from other drug classes, including calcium channel blockers, β-adrenergic receptor agonists/antagonists, and muscarinic acetylcholine receptor agonists/antagonists (Figure 2D). Selected hits from different classes of drugs were validated in vitro (Table 1 and Figure S2). Finally, HTS identified drugs that were less known to interact with OCT1, including carvedilol[29] (an antihypertensive medication) and ethopropazine (an anti-Parkinsonian agent). Selected hits not known previously to interact with OCT1 were validated by determining their IC_{50} values in vitro (Figure 4). Analysis of the physicochemical properties showed that OCT1 ligands tend to have fewer hydrogen-bond donors and acceptors and are less

DOI: 10.1021/acs.jmedchem.6b01317
J. Med. Chem. 2017, 60, 2685−2696

Table 1. Summary of IC_{50} Values for Selected Inhibition Studies

name	IC_{50} (μM)	IC_{50} 95% confidence interval
ketoconazole	2.60	2.49 to 2.78
closantel	3.00	2.83 to 3.18
dobutamine	4.17	3.73 to 4.67
alfuzosin	14.87	11.92 to 18.54
erlotinib	16.24	11.34 to 23.26
carbetapentane	1.55	1.19 to 2.02
clotrimazole	11.97	9.97 to 14.38
bithionol	2.23	1.98 to 2.52
carvediolol	3.43	3.02 to 3.90
clonidine	18.98	15.82 to 22.77
trimethoprim	50.68	41.47 to 61.93
guanabenz	4.85	4.17 to 5.64
pyrimethamine	13.57	10.74 to 17.14
dichlorophene	8.41	6.61 to 10.69
imipramine	7.95	5.91 to 10.68
cloperastine	14.89	14.00 to 15.83
dextromethorphan	10.45	8.66 to 12.61
propafenone	15.54	14.04 to 17.20
tacrine	21.72	18.77 to 25.14
ethopropazine	20.46	18.31 to 22.86
nitroprusside	43.84	38.08 to 50.46
sunitinib	6.10	5.47 to 6.79
desipramine	9.18	8.08 to 10.41
doxepin	11.19	9.89 to 12.66
camylofine	9.12	8.03 to 10.36
thiamine	4354	3704 to 5119

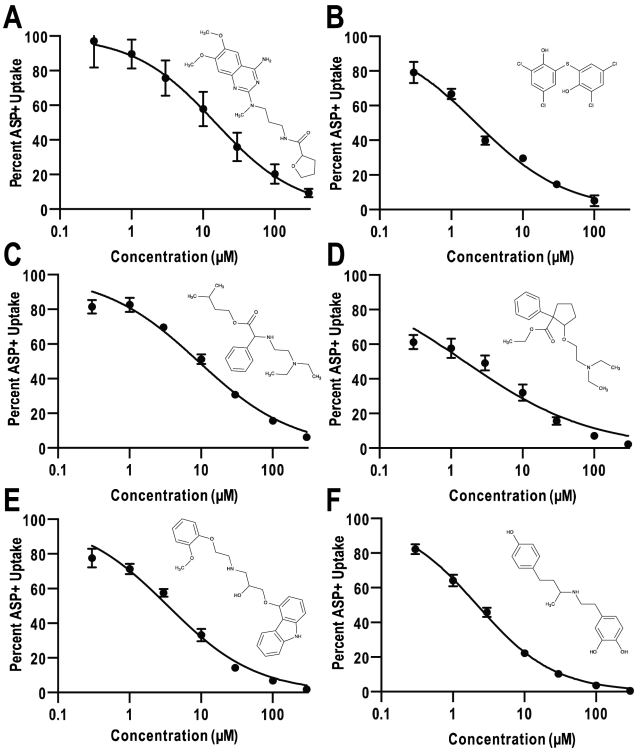

Figure 4. Selected inhibition studies of previously unknown OCT1 ligands and their estimated half-maximal inhibitory concentrations (IC_{50}), with 95% confidence limits in parentheses. (A) Alfuzosin, an α_1-adrenergic receptor antagonist. IC_{50} = 14.9 (11.9; 18.5) μM. (B) Bithionol, an anthelmintic. IC_{50} = 2.2 (2.0; 2.5) μM. (C) Camylofine, an antimuscarinic. IC_{50} = 9.1 (8.0; 10.4) μM. (D) Carbetapentane, an antitussive. IC_{50} = 1.6 (1.2; 2.0) μM. (E) Carvedilol, a nonselective β/α_1-adrenergic receptor antagonist. IC_{50} = 3.4 (3.0; 3.9) μM. (F) Dobutamine, a sympathomimetic. IC_{50} = 4.17 (3.73; 4.67) μM. Each data point represents mean ± SD, n = 6.

polar but more lipophilic than nonligands (Figure 5). As expected, ligands were more likely to be positively charged (Figure 5).

Prediction of Competitive Ligands. Thirty of the 1780 compounds in the library were identified as ligands by both virtual screening and HTS. Because docking was performed against the predicted binding site, we hypothesize that it can only identify competitive inhibitors or substrates. In contrast, HTS can identify both competitive and noncompetitive inhibitors or substrates. Thus, the 30 compounds that were identified with both methods are likely to be competitive inhibitors or even substrates. The remaining 137 compounds are hypothesized to be noncompetitive and/or mixed inhibitors of OCT1. It is also expected that this group may contain misclassified compounds. For example, inhibitors could be missed in HTS and thus be left out of our downstream analysis, resulting in false negatives. Alternatively, since docking was performed against a single conformation of a comparative transporter model, competitive inhibitors could have been misclassified by our protocol. We evaluated some of the compounds from this set of 137 inhibitors. Lineweaver–Burk plots were constructed for selected compounds in each class (Figure 6). Tacrine and ethopropazine, neither previously known to inhibit OCT1, were confirmed to be competitive inhibitors of ASP^+ and metformin uptake by OCT1 (Figures 6A,B and S3). Furthermore, we assessed the relative competitiveness of these inhibitors by calculating K_{is} (the dissociation constant for the transporter–inhibitor complex) and K_{ii} (the dissociation constant for the transporter–substrate–inhibitor complex) using previously published methods.[30] The ratios of K_{ii} and K_{is} for 14 compounds are summarized in Table S2. A larger K_{ii}/K_{is} value indicates a mode of inhibition that is relatively more competitive, whereas a lower K_{ii}/K_{is} value reflects less competitiveness. Our K_{ii}/K_{is} values ranged from 1.26 to 95.62 (Table S2). Thiamine had the highest value of K_{ii}/K_{is}, which indicated that it competitively inhibits ASP^+ uptake. In addition, thiamine has been validated as an OCT1 substrate in our previous publication.[2] Among the 14 compounds, compounds that were predicted to be competitive inhibitors resulted in relatively higher K_{ii}/K_{is}, whereas those that were predicted to be noncompetitive inhibitors had lower K_{ii}/K_{is} values.

Physicochemical Properties of Putative Competitive and Noncompetitive Inhibitors. We analyzed the physicochemical properties of 30 putative competitive and 137 noncompetitive ligands. Our analysis revealed that noncompetitive ligands were significantly larger and more hydrophobic than competitive ligands (Figure 3C), leading to the prediction that the two types of ligands might bind to different sites on the transporter.

In liver, several SLC transporters participate in uptake of drugs across the sinusoidal membrane into hepatocytes. A comparison of our HTS results with those for two other liver uptake transporters,[31,32] OATP1B1 (SLCO1B1) and OATP1B3 (SLCO1B3), allowed us to identify OCT1-selective versus pan inhibitors (i.e., compounds that inhibited transport of all three liver transporters). Fifty compounds inhibited the three liver transporters, whereas 112 inhibited OCT1 only. As

DOI: 10.1021/acs.jmedchem.6b01317
J. Med. Chem. 2017, 60, 2685–2696

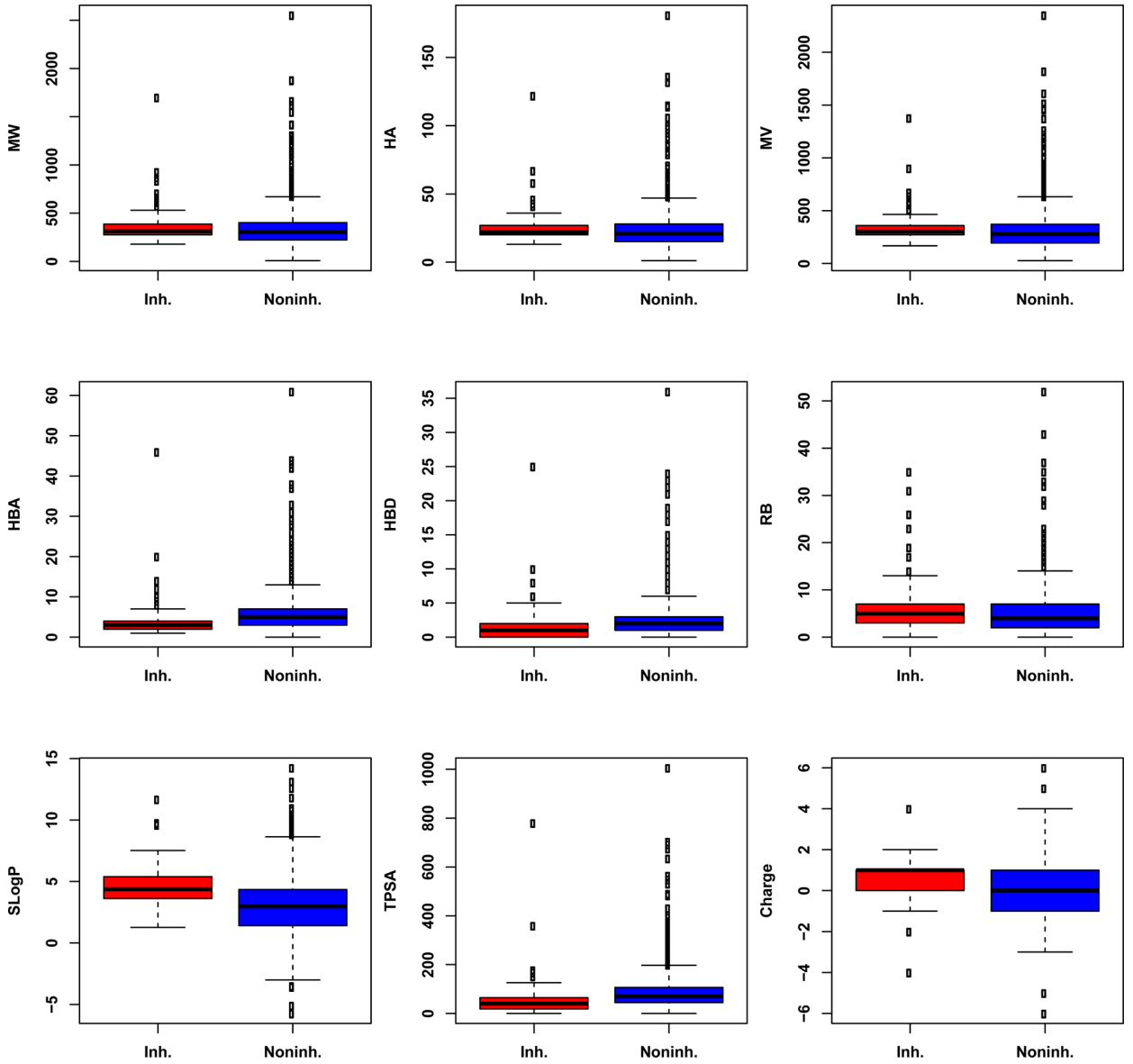

Figure 5. Differences in physicochemical properties of 167 inhibitors and 1613 noninhibitors. Shown are box plots of molecular weight (MW), number of heavy atoms (HA), molecular volume (MV), number of hydrogen-bond donors (HBD), number of hydrogen-bond acceptors (HBA), number of rotatable bonds (RB), SLogP, total polar surface area (TPSA), and charge at pH 7.4. Statistically significant differences were estimated using Student's *t* test. Distributions of inhibitors and noninhibitors were significantly different ($p < 0.05$) for HBD, HBA, SLogP, TPSA, and charge.

expected, differences in charge were significant (Student's *t* test, $p < 0.05$; Figure S4). Additionally, we found that OCT1 inhibitors were significantly smaller and less hydrophobic (Student's *t* test, $p < 0.05$). This result showed that multiway comparison of HTS data for several transporters can help in identifying compounds that are selective for a specific transporter and underscores the need for HTS of additional SLC transporters.

We next determined the fractions of inhibitors with different predicted inhibitory mechanisms among the OCT1-selective inhibitors and pan inhibitors (see the Supporting Information). Eight compounds inhibited OCT1 and OATP1B1 but not OATP1B3 (see the Supporting Information). Of these eight compounds, only ethacridine lactate was predicted to competitively inhibit OCT1. Likewise, only two out of 10 OCT1/OATP1B3 inhibitors were predicted to inhibit OCT1 competitively, and only two predicted competitive inhibitors were identified among 30 pan inhibitors. Interestingly, 22 out of 30 predicted competitive ligands of OCT1 (73%) were found among the OCT1-selective inhibitors. That is, these 22 were not inhibitors of OATP1B1 or OATP1B3. In contrast, only five out 30 predicted competitive ligands (16%) were also inhibitors of OATP1B1 and OATP1B3 (the remaining three compounds were not screened in OATP1B1/B3 HTS). This finding not only supports the accuracy of our comparative model but also highlights the importance of combining structure-guided ligand discovery with HTS. By combining experimental HTS with docking against a comparative model of OCT1, we can efficiently predict competitive OCT1-selective inhibitors with 73% accuracy. Therefore, a structure-guided approach greatly accelerates the identification of selective inhibitors and provides valuable information for drug−drug interaction studies compared with the conventional trial-and-error approach. Pan, OCT1/OATP1B1, and OCT1/OATP1B3 inhibitors

DOI: 10.1021/acs.jmedchem.6b01317
J. Med. Chem. 2017, 60, 2685−2696

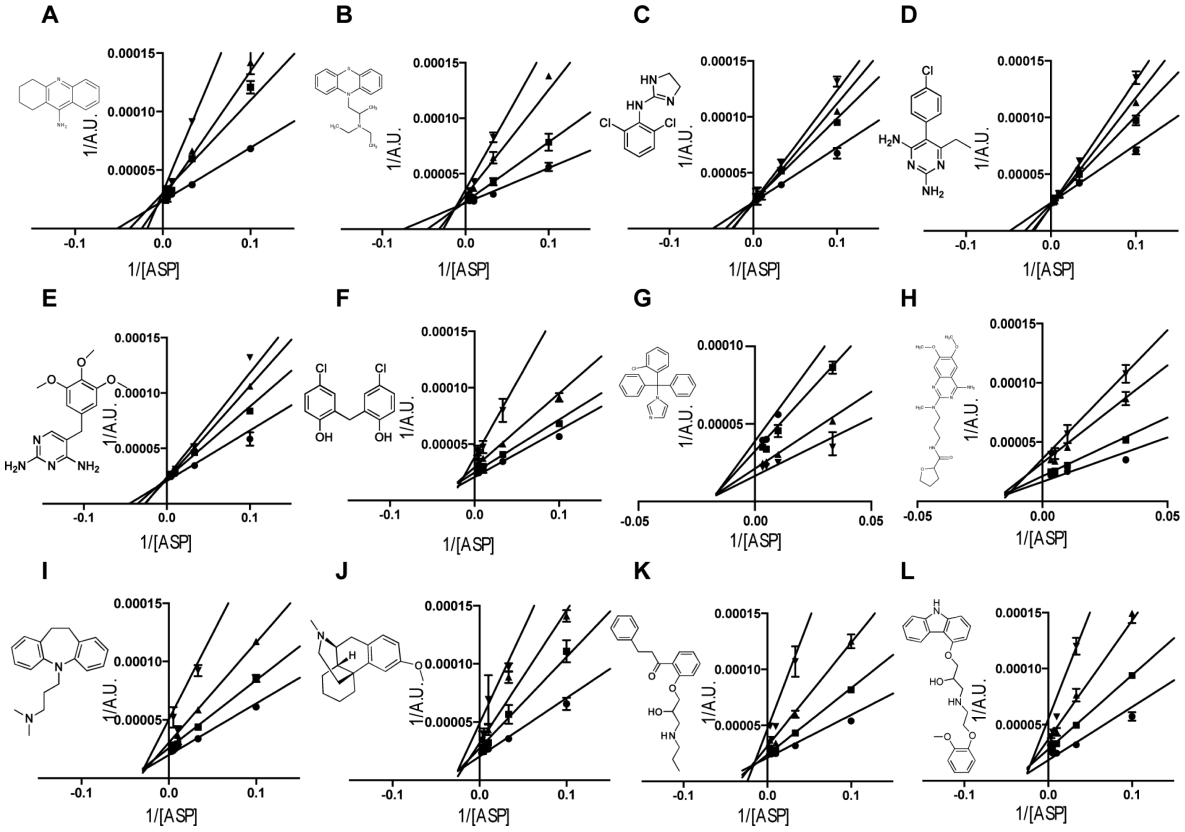

Figure 6. Lineweaver–Burk plots for discriminating between competitive and noncompetitive inhibitors of OCT1. The inhibitory effects on ASP^+ uptake by OCT1 with increasing concentrations of ASP^+ were measured at various concentrations (● < ■ < ▲ < ▼) of the following inhibitors: (A) tacrine; (B) ethopropazine; (C) clonidine; (D) pyrimethamine; (E) trimethoprim; (F) dichlorophene; (G) alfuzosin; (H) clotrimazole; (I) imipramine; (J) dextromethorphan; (K) propafenone; (L) carvedilol. Each data point represents mean ± SD, $n = 3$.

were enriched for noncompetitive inhibitors compared with OCT1-selective inhibitors.

Structure–Activity Modeling and Validation. Data from our OCT1 HTS experiment were used as a training set to construct a binary structure–activity relationship (SAR) model correlating molecular features of 1780 compounds from the Pharmacon library with their inhibitory activities, discretized into two classes: inhibitors and noninhibitors. The Random Forest (RF) algorithm[33] was employed to build an ensemble classifier (SAR-I). We evaluated the accuracy of the SAR-I model (i.e., the area under the receiver operating characteristic curve (auROC)) by 100 repeated cross-validation runs (Figure 7A). The average auROC of RF classifiers in this retrospective validation was 0.89 ± 0.3. This accuracy is comparable to the accuracies of retrospective validation of SAR models for other transporters.[24,34] In addition, we estimated the accuracy of RF-based SAR models in prospective validation as follows. First, we used molecular features and inhibitory outcomes of 183 compounds from a small previously published OCT1 inhibition screen[10] to develop a new SAR model (SAR-II). Next, SAR-II was utilized to predict the classes of the 1780 Pharmakon compounds. The auROC for this prospective validation was 0.84 (Figure 7B). Thus, the decrease in accuracy measures between retrospective and prospective validation was only 5%, strongly suggesting that our OCT1 SAR-I model is highly accurate (approximately 84%). We also used the SAR-II model to predict the sensitivity and specificity of the classifier at different cutoff values (Figure 7C). The sensitivity and specificity of the SAR-II model at a cutoff value of 0.6 were 92% and 43%, respectively; at a cutoff value of 0.4, they were 82% and 65%, respectively. Finally, the observed and SAR-II-predicted classification scores of the 1780 Pharmakon compounds were moderately correlated (Pearson correlation coefficient of 0.50; Figure 7D). These results suggest that SAR models can accurately predict OCT1 ligands by virtual screening.

Virtual Screening of Endogenous and Drug Metabolites. In addition to searching for OCT1 ligands among the 1780 prescription drugs, we applied our structure-based and SAR model methods to predict OCT1 ligands among a larger set of 29 332 endogenous and drug metabolites in the Human Metabolome Database (HMDB).[35] We found that 864 out of the 29 332 compounds (3%) docked favorably. We then computed ligand–OCT1 interaction values for the 864 compounds using the SAR-I model, allowing us to predict 146 competitive ligands. Among these 146 compounds, 1-benzyl-1,2,3,4-tetrahydroisoquinoline (1BnTIQ), an endogenous amine present at high levels in the cerebrospinal fluid of Parkinson's disease patients,[36,37] docked favorably against OCT1 (rank #14) and had SAR-I inhibition score of 0.48. 1BnTIQ inhibited OCT1 at 82.1 μM, and the Lineweaver–Burk plot confirmed that 1BnTIQ inhibited OCT1 competitively (Figure 8). This validation suggests that combined docking and SAR-I virtual screening can predict OCT1 metabolite ligands in addition to prescription drug ligands.

DOI: 10.1021/acs.jmedchem.6b01317
J. Med. Chem. 2017, 60, 2685–2696

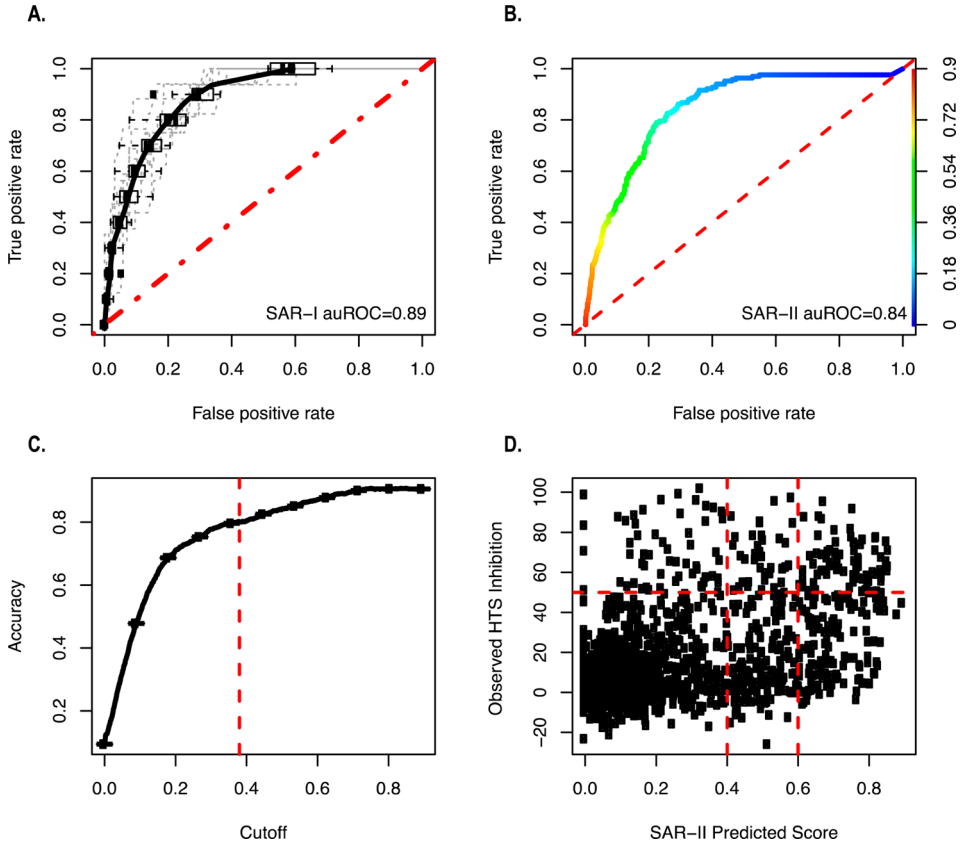

Figure 7. Results of structure–activity relationship modeling. (A) ROC curves for 100 retrospective cross-validation runs. The average ROC curve is shown in black. The ROC curve of a random classifier is shown as a red dotted line. (B) ROC curve for the SAR model tested in prospective validation of 1780 predicted inhibition values. The performances at different cutoff values (shown on the right *y*-axis) are indicated by rainbow colors. (C) Accuracy of classification of 1780 compounds using the SAR-II model as a function of cutoff. A cutoff of 0.38 is indicated by the red dotted line. (D) Observed vs predicted inhibition values for 1780 compounds. Two classification cutoffs are drawn vertically, and the HTS classification cutoff is drawn horizontally.

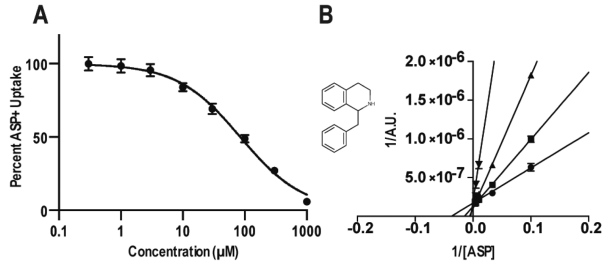

Figure 8. Inhibitory effects of 1BnTIQ on OCT1 transport. (A) 1BnTIQ inhibited ASP^+ uptake by OCT1, and the IC_{50} was determined to be 82.1 μM. (B) The inhibitory effect of 1BnTIQ on ASP^+ uptake by OCT1 indicated competitive inhibition. Each data point represents mean ± SD, n = 3.

■ DISCUSSION AND CONCLUSIONS

OCT1, a protein of great pharmacological interest, transports a wide array of drugs into and out of the liver and thus serves as a major determinant of drug metabolism and action. Because of its clinical importance, OCT1 has become a focus of many pharmacogenomics and drug interaction studies, which have prompted the EMA to recommend that all new drugs undergo in vitro testing to assess their liability to interact with OCT1.[8] The goals of the current study were (i) to develop robust computational models to predict the interaction of new molecular entities with OCT1 and (ii) to use a combination of experimental and computational approaches to identify prescription drug and metabolite ligands of OCT1. By combining in silico and in vitro approaches, we sought to gain information about whether a ligand binds competitively or noncompetitively on OCT1.

Three major findings emerged from the current studies. First, a comparative structural model of OCT1 successfully discriminated ligands from nonligands of the transporter. Second, by combining molecular docking and HTS approaches, we were indeed successful in determining whether a ligand interacts competitively or noncompetitively with the transporter. Third, we identified 30 and 137 prescription drugs as competitive and noncompetitive ligands of OCT1, respectively, including drugs not known to interact with the transporter. We now discuss each one of these findings in turn.

OCT1 Ligands Can Be Identified Accurately by Virtual Screening against an OCT1 Comparative Model. Accurate prediction of inhibitors and substrates of OCT1 is challenging. First, although several atomic structures have been resolved for bacterial members of the major facilitator superfamily of transporters, low sequence identity between bacterial homologues and human OCT1 casts doubt on the accuracy of comparative models built using these structures as templates.[16] Second, OCT1 is considered a polyspecific transporter that transports compounds of different sizes and

DOI: 10.1021/acs.jmedchem.6b01317
J. Med. Chem. 2017, 60, 2685–2696

molecular features. For example, OCT1 mediates the uptake of compounds ranging from small cations such as tetraethylammonium to monoamines (metformin), chemotherapy drugs (oxaliplatin), and hormone-like lipid compounds (prostaglandin E1).[4,38−40] This broad specificity may result in inaccurate docking and SAR models. For example, ligand-based models may underpredict ligands, especially in chemical spaces unsampled by the training set. Similarly, docking generally does not consider multiple binding sites, which are characteristic of polyspecific transporters. Finally, docking also depends on the accuracy of the target structure, and therefore, a combination of several computational and experimental validation experiments should be performed to ascertain the applicability of a homology model for docking.

Here we built a comparative model of human OCT1 in an inward-facing occluded conformation using a recently determined structure of its eukaryotic homologue, a phosphate transporter from *Piriformospora indica* (PiPT).[18] We confirmed that 80% of the known structurally diverse substrates can be docked favorably against the predicted binding site (Table S1). Three compounds that had unfavorable docking scores against this binding site had steric clashes with side chains of the binding cavity, underscoring the need to model transporters in alternative conformations. Unfortunately, there are no template structures for alternative conformations of OCT1, and molecular dynamics simulations still lack computing power to model conformational changes of transporters. The average pairwise Tanimoto coefficient of substrates used to validate the predicted binding site was 0.33, indicating that the compounds were structurally unrelated (Figure S5). In an unbiased validation of the OCT1 comparative model, we docked 1780 compounds from the Pharmakon library and validated 70% of the predicted binders and nonbinders in vitro. Previous SAR and pharmacophore models of OCT1−ligand interactions identified hydrophobicity and charge as the main physicochemical properties required for inhibition.[10,41,42] Our screening results confirmed that charge and hydrophobicity are positively correlated with the inhibitory activity of compounds (Figure 5). In addition, ligands had fewer hydrogen-bond donors and acceptors and were less polar than nonligands.

A Combination of Virtual Screening and HTS Can Determine Whether a Ligand Binds Competitively or Noncompetitively. It has been frequently assumed that inhibition of SLC-mediated transport is primarily competitive, although some recent studies have challenged this assumption by showing that competitive, noncompetitive, and mixed-type inhibition can also occur.[11,43−45] The International Transporter Consortium recently pointed out that the lack of understanding of inhibition mechanisms remains a limiting factor in transporter studies in drug development.[46] We showed that inhibitors of OCT1-mediated ASP^+ transport can be divided into two groups on the basis of their docking scores against the OCT1 model. Predicted competitive inhibitors of ASP^+ transport are compounds that are identified by experimental screening as well as predicted by virtual screening against the predicted substrate binding site; our assay and calculation do not distinguish between competitive inhibitors and substrates. In contrast, predicted noncompetitive inhibitors are compounds that are identified by experimental screening as well as predicted not to bind by virtual screening. Competitive ligands were significantly smaller and less hydrophobic than the noncompetitive ligands (Figure 3C). Because we modeled OCT1 in an inward-facing occluded conformation, we predict competitive ligands from only those compounds that fit into the compact translocation cavity. In addition, a broad range of K_{ii}/K_{is} values (Table S2) suggested various degrees of competitiveness among these inhibitors. Some of the inhibitors may bind to another binding cavity or to alternative OCT1 conformations, and these will not be predicted as competitive ligands by our docking approach. Furthermore, interactions with OCT1 have been shown to be ligand-dependent.[11] We used ASP^+ as our primary probe substrate in this study, but the mechanism of ligand-dependent interaction will need to be further investigated.

Additionally, we showed that 87% of predicted competitive ligands were selective for OCT1. In contrast, only 13% of predicted competitive ligands were identified among inhibitors of the three hepatic uptake transporters OCT1, OATP1B1, and OATP1B3. This result provides further confidence in the accuracy of the comparative model and its ability to predict competitive ligands.

To predict competitive ligands in a large virtual library of potential ligands, we combined the SAR model (built using our HTS data) and docking against a comparative OCT1 model. Indeed, 146 putative competitive ligands among endogenous and exogenous metabolites in the HMDB library were predicted; one of them, 1BnTIQ, was experimentally tested and validated (Figure 8). 1BnTIQ is an endogenous amine detected in human cerebrospinal fluid that accumulates in patients with Parkinson's disease[36] and is able to induce parkinsonism in both mice and monkeys.[47,48] 1BnTIQ inhibits complex I in the mitochondria and induces dopaminergic death in the same manner as MPP^+, a neurotoxin also known to induce parkinsonism. Structurally similar to MPP^+, 1BnTIQ is hydrophilic and requires an uptake mechanism to enter cells. A likely uptake mechanism is suggested by our identification of 1BnTIQ as an OCT1 ligand. While promising, our modeling method has low specificity, resulting in a large number of false positives. The modeling could be improved by docking against alternative conformations of the transporter once additional template structures become available.

Novel OCT1 Inhibitors Can Be Identified by HTS. Because of the critical role OCT1 plays in drug disposition and response, efforts have been made to identify and characterize OCT1 inhibitors. For example, 20 pharmacologically diverse antidepressants and 14 antipsychotics were screened using an OCT1-mediated radiolabeled MPP^+ uptake assay, identifying drugs that could potentially inhibit 50% or more OCT1 activity in the brain.[9] In another study, 191 drugs from various sources were compiled, followed by a medium-throughput identification of 62 inhibitors.[10]

In this study, we conducted an extensive HTS of 1780 drugs that have reached at least clinical trials in the United States or are marketed in Europe and/or Asia. We were able to confirm most of the previously known inhibitors. We also estimate that we identified at least 100 compounds previously unknown to interact with the transporter. Moreover, we grouped the identified OCT1 ligands into therapeutic classes, including tricyclic antidepressants, antihistamines, steroids, and α-adrenergic receptor agonists, all of which were previously reported to be more likely to interact with OCT1.[10] Our HTS also identified additional drug classes that were enriched in OCT1 ligands, including β-adrenergic receptor agonists/antagonists, calcium channel blockers, and muscarinic acetylcholine receptor agonists/antagonists. Among the inhibitors identified by HTS, selected compounds were validated by

DOI: 10.1021/acs.jmedchem.6b01317
J. Med. Chem. 2017, 60, 2685−2696

determining their IC_{50} values (Figure 4 and Table 1). Five of them (carbetapentane, carvedilol, erlotinib, griseofulvin, and ketoconazole) had IC_{50} values that were at least 10% of their maximum plasma concentrations achieved after therapeutic doses of the drug (Table 2). These estimates suggest the possibility of clinical drug−drug interactions with OCT1 substrates. Furthermore, OCT1 inhibitors may potentially have beneficial effects on hepatic steatosis.[2] With the exception of erlotinib and ketoconazole, the drugs noted here were newly identified OCT1 ligands. We also estimated their IC_{50} values for mouse OCT1 and two other human SLC uptake transporters (OCT2 and MATE1) (Table S3).

Table 2. Identified OCT1 Inhibitors That Could Cause Drug−Drug Interactions

name	IC_{50} (μM)[a]	C_{MAX} (μM)[b]	$C_{Portal\ Vein}$ (μM)[c]	C_{MAX}/IC_{50}
carbetapentane	1.6	0.2	N.A.	0.12
carvedilol	3.4	0.4	0.7	0.12
erlotinib	16.2	4.8	7.0	0.30
griseofulvin	7.3	4.5	4.6	0.62
ketoconazole	2.6	6.6	10.0	2.54

[a]IC_{50} is the estimated half-maximal inhibitory concentration (see the Experimental Section). [b]C_{MAX} values were obtained from http://www.micromedexsolutions.com/. [c]$C_{Portal\ Vein}$ values were calculated using the equation described previously.[60]

In conclusion, we have developed a comparative structural model of OCT1 that discriminates ligands from nonligands and used it together with an in vitro HTS assay. By combining the two approaches, we were able to predict whether a ligand binds competitively or noncompetitively. The structure-guided approach also accurately predicted inhibitors specific to OCT1 rather than two other hepatic drug transporters, OATP1B1 and OATP1B3. Finally, we conducted a virtual screen against a metabolite library using both comparative and SAR models built from HTS data and accurately identified and validated the parkinsonism-producing neurotoxin 1BnTIQ as a competitive inhibitor of OCT1.

EXPERIMENTAL SECTION

Chemicals. The MicroSource Pharmakon compound library (Gaylordsville, CT) was obtained through the Small Molecule Discovery Center at the University of California, San Francisco (San Francisco, CA). 4-(4-(Dimethylamino)styryl)-*N*-methylpyridinium iodide was purchased from Molecular Probes (Grand Island, NY). All other chemicals were purchased from Sigma-Aldrich (St. Louis, MO). All chemicals used in the studies were purchased from commercial vendors and had purities of 98% or higher. All cell culture media and supplements were purchased from Life Technologies (Carlsbad, CA), except for fetal bovine serum, which was purchased from GE Healthcare Life Sciences (South Logan, UT).

Cell Culture. Human embryonic kidney (HEK-293) cell line stably overexpressing OCT1 was established previously in our laboratory.[2] The cells were maintained in Dulbecco's Modified Eagle's Medium (DMEM H-21) supplemented with hygromycin B (75 μg/mL), penicillin (100 units/mL), streptomycin (100 mg/mL), and 10% fetal bovine serum in a humidified atmosphere with 5% CO_2 at 37 °C.

In Vitro Uptake Studies. HEK-293 cells overexpressing OCT1 were seeded in black, clear-bottom, poly(D-lysine)-coated 96-well plates (Greiner Bio-One, Monroe, NC) and allowed to grow for 48 h until approximately 90% confluency. For uptake kinetics studies, cells were incubated with Hank's balanced salt solution (HBSS) containing serial dilution of ASP^+ for 2 min at 37 °C. At the end of the experiments, the media were aspirated, and the cells were washed twice with ice-cold HBSS containing 50 μM spironolactone. The K_m and V_{max} were calculated by fitting the data to the Michaelis−Menten equation. For time course studies, cells were incubated with HBSS containing 2 μM ASP^+ at 37 °C. At various time points, the experiment was stopped as previously described. For IC_{50} determination, cells were incubated with HBSS containing 2 μM ASP^+ and serial dilution of inhibitors for 2 min at 37 °C. IC_{50} was determined using appropriate curve fitting. For Lineweaver−Burk plots, cells were incubated with HBSS containing serial dilution of ASP^+ and the inhibitor of interest at four different fixed concentrations for 2 min at 37 °C. The reciprocal value of ASP^+ uptake at each inhibitor concentration was fitted with linear regression. The signal of ASP^+ was measured using an Analyst AD plate reader (Molecular Devices, Sunnyvale, CA) with excitation and emission filters tuned at wavelengths of 485 and 585 nm, respectively. All statistical analysis and curve fitting were done using GraphPad Prism software (La Jolla, CA).

High-Throughput Screening. The high-throughput screen was performed at the Small Molecule Discovery Center at the University of California, San Francisco. HEK-293 cells overexpressing OCT1 were seeded in black, clear bottom, poly(D-lysine)-coated 96-well plates (Greiner Bio-One) and allowed to grow for 48 h until approximately 90% confluency using methods established previously.[24] Cells were incubated with HBSS containing 2 μM ASP^+ and 20 μM test compound at ambient temperature for approximately 2 min. At the end of the experiment, media were aspirated, and cells were washed twice with HBSS containing 50 μM spironolactone. Nonspecific transport was determined in wells on each assay plate using 100 μM spironolactone as the OCT1 inhibitor. The screen was carried out with a Biomek FXp liquid handler (Beckman Coulter, Brea, CA). Fluorescence was measured as previously described.

OCT1 Structure Modeling and Docking. Human OCT1 was modeled using the 2.9 Å structure of a high-affinity phosphate transporter from *Piriformospora indica* (PiPT) crystallized in an inward-facing occluded state with bound phosphate.[13] The template was selected on the basis of the shared MFS fold assignment,[47] structure quality, sequence similarity to OCT1, and ligand-bound conformation. The sequence alignment was obtained by a manual refinement of gaps in the output from the PROMALS3D[49] and MUSCLE[50] servers (Figure S6). One hundred models were generated using the "automodel" class of MODELLER 9.14 (https://salilab.org/modeller/contact.html) and the normalized discrete optimized protein energy (zDOPE) potential.[14] The top-scoring model was used to predict putative binding sites with the FTMap web server.[51] Two of the predicted binding sites were identified in the translocation cavity between the two domains.[13] ASP^+ probe substrate was docked against the two binding sites with UCSF DOCK 3.6.[52,53] The size of the docking box was 38 Å × 40 Å × 38 Å. The pose with the best docking score was used as the template for another round of comparative modeling by MODELER 9.14, generating 100 new models of OCT1. Each of the models was then evaluated for ligand enrichment from a set of challenging decoys based on enrichment curves and corresponding logAUC values.[54] Sixty decoys were generated using the Database of Useful Decoys (DUD)[55] for each of the selected experimentally validated substrates of OCT1. The best-scoring model was used for subsequent virtual screening. Compounds in the Pharmakon library were downloaded from the ZINC database[56] and docked against the predicted binding site on the comparative model using UCSF DOCK 3.6. A negative DOCK score predicts a favorable interaction with the transporter, while a positive score predicts an unfavorable (or unlikely) intermolecular interaction. Normalized docking scores were computed by subtracting the average docking score of all compounds (including the nonbinders) from the docking score of an individual compound and dividing by the standard deviation of all docking scores. The PAINS-Remover online web server was used to check Pharmkon compounds for the likelihood of interference in screening.[57] None of the 1780 compounds was reported as a pan-assay interference compound.

Structure−Activity Relationship Modeling of OCT1 Inhibition. Two-dimensional (2D) structure files of the 1780 compounds

DOI: 10.1021/acs.jmedchem.6b01317
J. Med. Chem. 2017, 60, 2685−2696

from the Pharmakon library were also downloaded from the ZINC database,[56] and 2900 molecular descriptors and the charge at pH 7.4 for each compound were computed using PaDEL software[53] and cxcalc (ChemAxon; http://www.chemaxon.com), respectively. Non-informative descriptors (i.e., molecular descriptors with near-zero variance and redundant descriptors defined by a correlation higher than 0.95 to an accepted descriptor) were removed. Next, the information content and correlation between descriptor values and percent inhibition of 1780 compounds were computed with the cfs filtering algorithm in the FSelector package[58] in R, and the 21 most informative descriptors were retained for further modeling. These descriptors are Moreau−Broto autocorrelation descriptors based on atomic polarizability (ATSp4), number of doubly bound carbons bound to two other carbons (C2SP2), count of atom-type E-State >CH− (nsssCH), sum of E-States for weak hydrogen-bond acceptors (SwHBa), sum of E-State descriptors of strength for potential hydrogen bonds of path length 7 (SHBint7), sum of atom-type E-State =C< (SdssC), minimum E-State descriptors of strength for potential hydrogen bonds of path length 8 (minHBint8), minimum atom-type H E-State −OH (minHsOH), minimum atom-type E-State $-CH_3$ (minsCH3), minimum atom-type E-State $-CH_2-$ (minssCH2), minimum atom-type E-State >C< (minsssC), minimum atom-type E-State $>NH^+-$ (minsssN), maximum E-States for (strong) hydrogen-bond acceptors (maxHBa), maximum E-State descriptors of strength for potential hydrogen bonds of path length 2 (maxHBint2), maximum atom-type E-State =C< (maxdssC), a measure of electronegative atom count (ETA_Epsilon_1), a measure of hydrogen-bonding propensity of the molecules and/or polar surface area (ETA_Psi_1), a measure of electronegative atom count of the molecule relative to molecular size (ETA_BetaP_s), Mannhold LogP (MLogP), logarithm of the calculated octanol/water partition coefficient (XLog), and charge (Charge). Percent inhibition values determined by HTS were discretized into two outcomes: values of at least 50% were mapped to "1" (i.e., ligand), and values of less than 50%, including negative values, were mapped to "0" (i.e., nonligand). Binary SAR models were built with the RF algorithm.[33] Their accuracy was estimated using a double-loop fivefold cross-validation[24] protocol in the caret package in R. To evaluate the accuracy of the models, the average area under the receiver operating characteristic curve (auROC) was computed from 100 repeated double-loop cross-validation runs. For prospective validation, 21 molecular descriptors for 183 compounds[10] were computed (Supporting Information), and SAR models were optimized by repeated fivefold cross-validation. The model was employed to predict inhibition values for the 1780 compounds in the Pharmakon library.

Virtual Screening against HMDB Library. For virtual screening, molecular structure files of the HMDB compounds were downloaded from the ZINC database,[56] and 21 molecular features (Supporting Information) were computed for each compound. The ligand score ranging between 0 and 1 was computed for each compound by SAR-I. Compounds with ligand scores higher than 0.4 were labeled as ligands. In parallel, each compound was docked against predicted binding sites on the OCT1 transporter using UCSF DOCK 3.6. Normalized docking scores were computed by subtracting the average docking score of all docked compounds from the docking score of a compound and dividing by the standard deviation of all docking scores. Compounds with normalized docking scores less than −1 and ligand scores greater than 0.4 were labeled as competitive inhibitors.

Pairwise Compound Similarity Computation and Clustering. The MayaChemTools (http://www.mayachemtools.org) package was used to compute 2D extended connectivity fingerprints (ECFPs) and pairwise Tanimoto coefficients. The *hclust* function from the *stats* library[59] was used to perform hierarchical compound clustering.

■ ASSOCIATED CONTENT

Supporting Information

The Supporting Information is available free of charge on the ACS Publications website at DOI: 10.1021/acs.jmedchem.6b01317.

Summary of 15 substrates used to validate OCT1 docking site, the ratios of K_{ii} and K_{is} for selective inhibitors, comparison of IC_{50} values for OCT1 inhibitors in four different cell lines, effect of thiamine on the uptake of ASP^+ by OCT1, selected inhibition studies of OCT1 ligands and their estimated IC_{50} values, Lineweaver−Burk plots for discriminating between competitive and noncompetitive inhibitors of OCT1-mediated metformin uptake, differences in physicochemical properties of OCT1-selective and pan inhibitors, 2D dissimilarity clustering of 15 known substrates of OCT1, and pairwise sequence alignment of PiPT and OCT1 (PDF)

Full list of Pharmakon library compounds with SMILES strings, ASP^+ inhibition data, and docking scores; list of HMDB compounds with docking ranks; OCT1, OATP1B1, and OATP1B3 inhibition results; names and descriptions of the 21 descriptors used in SAR modeling; and slope and intercept data (XLSX)

OCT1 comparative model (PDB)

■ AUTHOR INFORMATION

Corresponding Author

*E-mail: Kathy.giacomini@ucsf.edu.

ORCID

Natalia Khuri: 0000-0001-9031-8124

Andrej Sali: 0000-0003-0435-6197

Kathleen M. Giacomini: 0000-0001-8041-5430

Present Addresses

[#]E.C.C.: Department of Metabolism and Pharmacokinetics, Genentech, South San Francisco, CA 94080.

[▽]N.K.: Department of Bioengineering, Stanford University, Stanford, CA 94305.

Author Contributions

[○]E.C.C., N.K., and X.L. contributed equally to this work. E.C.C., N.K., X.L., Y.H., A. Sali, and K.M.G. designed the research; E.C.C., N.K., X.L., A. Stecula, H.-C.C., and S.W.Y. conducted the experiments; E.C.C., N.K., X.L., A. Stecula, H.-C.C., A. Sali, and K.M.G. analyzed the data; E.C.C., N.K., X.L., A. Sali, and K.M.G. wrote the paper.

Notes

The authors declare no competing financial interest.

■ ACKNOWLEDGMENTS

We thank Dr. Robert M. Stroud, Dr. Ethan Geier, and Dr. Avner Schlessinger for helpful discussions and Steven Chen from the UCSF Small Molecule Discovery Center for help with the assay automation. The project was supported by grants from the National Institutes of Health (R01 GM54762, U54 GM62529, P01 GM71790, and P01 A135707 to A. Sali; U19 GM61390 and R01 GM117163 to K.M.G.; T32 GM007175 to E.C.C., X.L., and A. Stecula; T32 GM008284 to N.K.; 2R44GM086970-03A1 to Y.H.). We also acknowledge hardware gifts from Intel and IBM.

■ ABBREVIATIONS USED

HTS, high-throughput screening; SAR, structure−activity relationship; ASP^+, 4-Di-1-ASP; OCT1, organic cation transporter 1; SLC, solute carrier; TMH, transmembrane helix; HMDB, Human Metabolome Database; 1BnTIQ, 1-benzyl-

DOI: 10.1021/acs.jmedchem.6b01317
J. Med. Chem. 2017, 60, 2685−2696

1,2,3,4-tetrahydroisoquinoline; HEK-293, human embryonic kidney cell line

REFERENCES

(1) Boxberger, K. H.; Hagenbuch, B.; Lampe, J. N. Common Drugs Inhibit Human Organic Cation Transporter 1 (OCT1)-Mediated Neurotransmitter Uptake. *Drug Metab. Dispos.* **2014**, *42* (6), 990−995.

(2) Chen, L.; Shu, Y.; Liang, X.; Chen, E. C.; Yee, S. W.; Zur, A. A.; Li, S.; Xu, L.; Keshari, K. R.; Lin, M. J.; Chien, H.-C.; Zhang, Y.; Morrissey, K. M.; Liu, J.; Ostrem, J.; Younger, N. S.; Kurhanewicz, J.; Shokat, K. M.; Ashrafi, K.; Giacomini, K. M. OCT1 Is a High-Capacity Thiamine Transporter That Regulates Hepatic Steatosis and Is a Target of Metformin. *Proc. Natl. Acad. Sci. U. S. A.* **2014**, *111* (27), 9983−9988.

(3) Kell, D. B. Implications of Endogenous Roles of Transporters for Drug Discovery: Hitchhiking and Metabolite-Likeness. *Nat. Rev. Drug Discovery* **2016**, *15* (2), 143.

(4) Shu, Y.; Sheardown, S. A.; Brown, C.; Owen, R. P.; Zhang, S.; Castro, R. A.; Ianculescu, A. G.; Yue, L.; Lo, J. C.; Burchard, E. G.; Brett, C. M.; Giacomini, K. M. Effect of Genetic Variation in the Organic Cation Transporter 1 (OCT1) on Metformin Action. *J. Clin. Invest.* **2007**, *117* (5), 1422−1431.

(5) Tzvetkov, M. V.; Saadatmand, A. R.; Lötsch, J.; Tegeder, I.; Stingl, J. C.; Brockmöller, J. Genetically Polymorphic OCT1: Another Piece in the Puzzle of the Variable Pharmacokinetics and Pharmacodynamics of the Opioidergic Drug Tramadol. *Clin. Pharmacol. Ther.* **2011**, *90* (1), 143−150.

(6) Cho, S. K.; Kim, C. O.; Park, E. S.; Chung, J.-Y. Verapamil Decreases the Glucose-Lowering Effect of Metformin in Healthy Volunteers. *Br. J. Clin. Pharmacol.* **2014**, *78* (6), 1426−1432.

(7) Giacomini, K. M.; Huang, S.-M.; Tweedie, D. J.; Benet, L. Z.; Brouwer, K. L. R.; Chu, X.; Dahlin, A.; Evers, R.; Fischer, V.; Hillgren, K. M.; Hoffmaster, K. A.; Ishikawa, T.; Keppler, D.; Kim, R. B.; Lee, C. A.; Niemi, M.; Polli, J. W.; Sugiyama, Y.; Swaan, P. W.; Ware, J. A.; Wright, S. H.; Yee, S. W.; Zamek-Gliszczynski, M. J.; Zhang, L. Membrane Transporters in Drug Development. *Nat. Rev. Drug Discovery* **2010**, *9* (3), 215−236.

(8) *Guideline on the Investigation of Drug Interactions*; European Medicines Agency: London, 2015.

(9) Haenisch, B.; Drescher, E.; Thiemer, L.; Xin, H.; Giros, B.; Gautron, S.; Bönisch, H. Interaction of Antidepressant and Antipsychotic Drugs with the Human Organic Cation Transporters hOCT1, hOCT2 and hOCT3. *Naunyn-Schmiedeberg's Arch. Pharmacol.* **2012**, *385* (10), 1017−1023.

(10) Ahlin, G.; Karlsson, J.; Pedersen, J. M.; Gustavsson, L.; Larsson, R.; Matsson, P.; Norinder, U.; Bergström, C. A. S.; Artursson, P. Structural Requirements for Drug Inhibition of the Liver Specific Human Organic Cation Transport Protein 1. *J. Med. Chem.* **2008**, *51* (19), 5932−5942.

(11) Belzer, M.; Morales, M.; Jagadish, B.; Mash, E. A.; Wright, S. H. Substrate-Dependent Ligand Inhibition of the Human Organic Cation Transporter OCT2. *J. Pharmacol. Exp. Ther.* **2013**, *346* (2), 300−310.

(12) Koepsell, H. Polyspecific Organic Cation Transporters: Their Functions and Interactions with Drugs. *Trends Pharmacol. Sci.* **2004**, *25* (7), 375−381.

(13) Zhang, X.; Shirahatti, N. V.; Mahadevan, D.; Wright, S. H. A Conserved Glutamate Residue in Transmembrane Helix 10 Influences Substrate Specificity of Rabbit OCT2 (SLC22A2). *J. Biol. Chem.* **2005**, *280* (41), 34813−34822.

(14) Koepsell, H. Substrate Recognition and Translocation by Polyspecific Organic Cation Transporters. *Biol. Chem.* **2011**, *392* (1−2), 95−101.

(15) Gorboulev, V.; Shatskaya, N.; Volk, C.; Koepsell, H. Subtype-Specific Affinity for Corticosterone of Rat Organic Cation Transporters rOCT1 and rOCT2 Depends on Three Amino Acids Within the Substrate Binding Region. *Mol. Pharmacol.* **2005**, *67* (5), 1612−1619.

(16) Popp, C.; Gorboulev, V.; Müller, T. D.; Gorbunov, D.; Shatskaya, N.; Koepsell, H. Amino Acids Critical for Substrate Affinity of Rat Organic Cation Transporter 1 Line the Substrate Binding Region in a Model Derived From the Tertiary Structure of Lactose Permease. *Mol. Pharmacol.* **2005**, *67* (5), 1600−1611.

(17) Volk, C.; Gorboulev, V.; Kotzsch, A.; Müller, T. D.; Koepsell, H. Five Amino Acids in the Innermost Cavity of the Substrate Binding Cleft of Organic Cation Transporter 1 Interact with Extracellular and Intracellular Corticosterone. *Mol. Pharmacol.* **2009**, *76* (2), 275−289.

(18) Pedersen, B. P.; Kumar, H.; Waight, A. B.; Risenmay, A. J.; Roe-Zurz, Z.; Chau, B. H.; Schlessinger, A.; Bonomi, M.; Harries, W.; Sali, A.; Johri, A. K.; Stroud, R. M. Crystal Structure of a Eukaryotic Phosphate Transporter. *Nature* **2013**, *496* (7446), 533−536.

(19) Shen, M.-Y.; Sali, A. Statistical Potential for Assessment and Prediction of Protein Structures. *Protein Sci.* **2006**, *15* (11), 2507−2524.

(20) Eramian, D.; Eswar, N.; Shen, M.-Y.; Sali, A. How Well Can the Accuracy of Comparative Protein Structure Models Be Predicted? *Protein Sci.* **2008**, *17* (11), 1881−1893.

(21) Keller, T.; Egenberger, B.; Gorboulev, V.; Bernhard, F.; Uzelac, Z.; Gorbunov, D.; Wirth, C.; Koppatz, S.; Dötsch, V.; Hunte, C.; Sitte, H. H.; Koepsell, H. The Large Extracellular Loop of Organic Cation Transporter 1 Influences Substrate Affinity and Is Pivotal for Oligomerization. *J. Biol. Chem.* **2011**, *286* (43), 37874−37886.

(22) Schlessinger, A.; Wittwer, M. B.; Dahlin, A.; Khuri, N.; Bonomi, M.; Fan, H.; Giacomini, K. M.; Sali, A. High Selectivity of the Γ-Aminobutyric Acid Transporter 2 (GAT-2, SLC6A13) Revealed by Structure-Based Approach. *J. Biol. Chem.* **2012**, *287* (45), 37745−37756.

(23) Schlessinger, A.; Geier, E.; Fan, H.; Irwin, J. J.; Shoichet, B. K.; Giacomini, K. M.; Sali, A. Structure-Based Discovery of Prescription Drugs That Interact with the Norepinephrine Transporter, NET. *Proc. Natl. Acad. Sci. U. S. A.* **2011**, *108* (38), 15810−15815.

(24) Kido, Y.; Matsson, P.; Giacomini, K. M. Profiling of a Prescription Drug Library for Potential Renal Drug-Drug Interactions Mediated by the Organic Cation Transporter 2. *J. Med. Chem.* **2011**, *54* (13), 4548−4558.

(25) Zhang, J.-H.; Chung, T. D. Y.; Oldenburg, K. R. A Simple Statistical Parameter for Use in Evaluation and Validation of High Throughput Screening Assays. *J. Biomol. Screening* **1999**, *4* (2), 67−73.

(26) Carlsson, J.; Coleman, R. G.; Setola, V.; Irwin, J. J.; Fan, H.; Schlessinger, A.; Sali, A.; Roth, B. L.; Shoichet, B. K. Ligand Discovery From a Dopamine D3 Receptor Homology Model and Crystal Structure. *Nat. Chem. Biol.* **2011**, *7* (11), 769−778.

(27) Minematsu, T.; Iwai, M.; Umehara, K.-I.; Usui, T.; Kamimura, H. Characterization of Human Organic Cation Transporter 1 (OCT1/SLC22A1)- and OCT2 (SLC22A2)-Mediated Transport of 1-(2-Methoxyethyl)-2-Methyl-4,9-Dioxo-3-(Pyrazin-2-Ylmethyl)- 4,9-Dihydro-1H-Naphtho[2,3-D]Imidazolium Bromide (YM155 Monobromide), a Novel Small Molecule Survivin Suppressant. *Drug Metab. Dispos.* **2010**, *38* (1), 1−4.

(28) Bourdet, D. L.; Pritchard, J. B.; Thakker, D. R. Differential Substrate and Inhibitory Activities of Ranitidine and Famotidine Toward Human Organic Cation Transporter 1 (hOCT1; SLC22A1), hOCT2 (SLC22A2), and hOCT3 (SLC22A3). *J. Pharmacol. Exp. Ther.* **2005**, *315* (3), 1288−1297.

(29) Bachmakov, I.; Glaeser, H.; König, J. Einfluss Von B-Blockern Auf Den Transport Von Metformin Durch Den Hepatischen Aufnahmetransporter Für Organische Kationen OCT1. *Diabetologie und Stoffwechsel* **2009**, *4*, 274.

(30) Barr, J. T.; Jones, J. P. Inhibition of Human Liver Aldehyde Oxidase: Implications for Potential Drug-Drug Interactions. *Drug Metab. Dispos.* **2011**, *39* (12), 2381−2386.

(31) Gui, C.; Obaidat, A.; Chaguturu, R.; Hagenbuch, B. Development of a Cell-Based High-Throughput Assay to Screen for Inhibitors of Organic Anion Transporting Polypeptides 1B1 and 1B3. *Curr. Chem. Genomics* **2010**, *4*, 1−8.

(32) De Bruyn, T.; van Westen, G. J. P.; Ijzerman, A. P.; Stieger, B.; de Witte, P.; Augustijns, P. F.; Annaert, P. P. Structure-Based Identification of OATP1B1/3 Inhibitors. *Mol. Pharmacol.* **2013**, *83* (6), 1257−1267.

DOI: 10.1021/acs.jmedchem.6b01317
J. Med. Chem. 2017, 60, 2685−2696

(33) Svetnik, V.; Liaw, A.; Tong, C.; Culberson, J. C.; Sheridan, R. P.; Feuston, B. P. Random Forest: a Classification and Regression Tool for Compound Classification and QSAR Modeling. *J. Chem. Inf. Model.* **2003**, *43* (6), 1947−1958.
(34) Wittwer, M. B.; Zur, A. A.; Khuri, N.; Kido, Y.; Kosaka, A.; Zhang, X.; Morrissey, K. M.; Sali, A.; Huang, Y.; Giacomini, K. M. Discovery of Potent, Selective Multidrug and Toxin Extrusion Transporter 1 (MATE1, SLC47A1) Inhibitors Through Prescription Drug Profiling and Computational Modeling. *J. Med. Chem.* **2013**, *56* (3), 781−795.
(35) Wishart, D. S.; Jewison, T.; Guo, A. C.; Wilson, M.; Knox, C.; Liu, Y.; Djoumbou, Y.; Mandal, R.; Aziat, F.; Dong, E.; Bouatra, S.; Sinelnikov, I.; Arndt, D.; Xia, J.; Liu, P.; Yallou, F.; Bjorndahl, T.; Perez-Pineiro, R.; Eisner, R.; Allen, F.; Neveu, V.; Greiner, R.; Scalbert, A. HMDB 3.0–the Human Metabolome Database in 2013. *Nucleic Acids Res.* **2013**, *41* (D1), D801−D807.
(36) Kotake, Y. [Tetrahydroisoquinoline Derivatives as Possible Parkinson's Disease-Inducing Substances]. *Yakugaku Zasshi* **2002**, *122* (11), 975−982.
(37) Kotake, Y.; Tasaki, Y.; Makino, Y.; Ohta, S.; Hirobe, M. 1-Benzyl-1,2,3,4-Tetrahydroisoquinoline as a Parkinsonism-Inducing Agent: a Novel Endogenous Amine in Mouse Brain and Parkinsonian CSF. *J. Neurochem.* **1995**, *65* (6), 2633−2638.
(38) Zhang, L.; Schaner, M. E.; Giacomini, K. M. Functional Characterization of an Organic Cation Transporter (hOCT1) in a Transiently Transfected Human Cell Line (HeLa). *J. Pharmacol. Exp. Ther.* **1998**, *286* (1), 354−361.
(39) Zhang, S.; Lovejoy, K. S.; Shima, J. E.; Lagpacan, L. L.; Shu, Y.; Lapuk, A.; Chen, Y.; Komori, T.; Gray, J. W.; Chen, X.; Lippard, S. J.; Giacomini, K. M. Organic Cation Transporters Are Determinants of Oxaliplatin Cytotoxicity. *Cancer Res.* **2006**, *66* (17), 8847−8857.
(40) Kimura, H.; Takeda, M.; Narikawa, S.; Enomoto, A.; Ichida, K.; Endou, H. Human Organic Anion Transporters and Human Organic Cation Transporters Mediate Renal Transport of Prostaglandins. *J. Pharmacol. Exp. Ther.* **2002**, *301* (1), 293−298.
(41) Bednarczyk, D.; Ekins, S.; Wikel, J. H.; Wright, S. H. Influence of Molecular Structure on Substrate Binding to the Human Organic Cation Transporter, hOCT1. *Mol. Pharmacol.* **2003**, *63* (3), 489−498.
(42) Moaddel, R.; Ravichandran, S.; Bighi, F.; Yamaguchi, R.; Wainer, I. W. Pharmacophore Modelling of Stereoselective Binding to the Human Organic Cation Transporter (hOCT1). *Br. J. Pharmacol.* **2007**, *151* (8), 1305−1314.
(43) Harper, J. N.; Wright, S. H. Multiple Mechanisms of Ligand Interaction with the Human Organic Cation Transporter, OCT2. *Am. J. Physiol. Renal Physiol.* **2013**, *304* (1), F56−F67.
(44) Ekins, S.; Polli, J. E.; Swaan, P. W.; Wright, S. H. Computational Modeling to Accelerate the Identification of Substrates and Inhibitors for Transporters That Affect Drug Disposition. *Clin. Pharmacol. Ther.* **2012**, *92* (5), 661−665.
(45) Martínez-Guerrero, L. J.; Wright, S. H. Substrate-Dependent Inhibition of Human MATE1 by Cationic Ionic Liquids. *J. Pharmacol. Exp. Ther.* **2013**, *346* (3), 495−503.
(46) Tweedie, D.; Polli, J. W.; Berglund, E. G.; Huang, S. M.; Zhang, L.; Poirier, A.; Chu, X.; Feng, B. International Transporter Consortium. Transporter Studies in Drug Development: Experience to Date and Follow-Up on Decision Trees From the International Transporter Consortium. *Clin. Pharmacol. Ther.* **2013**, *94* (1), 113−125.
(47) Abe, K.; Taguchi, K.; Wasai, T.; Ren, J.; Utsunomiya, I.; Shinohara, T.; Miyatake, T.; Sano, T. Biochemical and Pathological Study of Endogenous 1-Benzyl-1,2,3,4-Tetrahydroisoquinoline-Induced Parkinsonism in the Mouse. *Brain Res.* **2001**, *907* (1−2), 134−138.
(48) Kotake, Y.; Yoshida, M.; Ogawa, M.; Tasaki, Y.; Hirobe, M.; Ohta, S. Chronic Administration of 1-Benzyl-1,2,3,4-Tetrahydroisoquinoline, an Endogenous Amine in the Brain, Induces Parkinsonism in a Primate. *Neurosci. Lett.* **1996**, *217* (1), 69−71.
(49) Pei, J.; Kim, B.-H.; Grishin, N. V. PROMALS3D: a Tool for Multiple Protein Sequence and Structure Alignments. *Nucleic Acids Res.* **2008**, *36* (7), 2295−2300.
(50) Edgar, R. C. MUSCLE: Multiple Sequence Alignment with High Accuracy and High Throughput. *Nucleic Acids Res.* **2004**, *32* (5), 1792−1797.
(51) Kozakov, D.; Grove, L. E.; Hall, D. R.; Bohnuud, T.; Mottarella, S. E.; Luo, L.; Xia, B.; Beglov, D.; Vajda, S. The FTMap Family of Web Servers for Determining and Characterizing Ligand-Binding Hot Spots of Proteins. *Nat. Protoc.* **2015**, *10* (5), 733−755.
(52) Huang, N.; Shoichet, B. K.; Irwin, J. J. Benchmarking Sets for Molecular Docking. *J. Med. Chem.* **2006**, *49* (23), 6789−6801.
(53) Yap, C. W. PaDEL-Descriptor: an Open Source Software to Calculate Molecular Descriptors and Fingerprints. *J. Comput. Chem.* **2011**, *32* (7), 1466−1474.
(54) Fan, H.; Irwin, J. J.; Webb, B. M.; Klebe, G.; Shoichet, B. K.; Sali, A. Molecular Docking Screens Using Comparative Models of Proteins. *J. Chem. Inf. Model.* **2009**, *49* (11), 2512−2527.
(55) Mysinger, M. M.; Carchia, M.; Irwin, J. J.; Shoichet, B. K. Directory of Useful Decoys, Enhanced (DUD-E): Better Ligands and Decoys for Better Benchmarking. *J. Med. Chem.* **2012**, *55* (14), 6582−6594.
(56) Irwin, J. J.; Shoichet, B. K. ZINC—A Free Database of Commercially Available Compounds for Virtual Screening. *J. Chem. Inf. Model.* **2005**, *45* (1), 177−182.
(57) Baell, J. B.; Holloway, G. A. New Substructure Filters for Removal of Pan Assay Interference Compounds (PAINS) From Screening Libraries and for Their Exclusion in Bioassays. *J. Med. Chem.* **2010**, *53* (7), 2719−2740.
(58) Cheng, T.; Wang, Y.; Bryant, S. H. FSelector: a Ruby Gem for Feature Selection. *Bioinformatics* **2012**, *28* (21), 2851−2852.
(59) R Development Core Team. *R: A Language and Environment for Statistical Computing*; The R Foundation for Statistical Computing: Vienna, Austria, 2011; available online at http://www.R-project.org/.
(60) Ito, K.; Chiba, K.; Horikawa, M.; Ishigami, M.; Mizuno, N.; Aoki, J.; Gotoh, Y.; Iwatsubo, T.; Kanamitsu, S.-I.; Kato, M.; Kawahara, I.; Niinuma, K.; Nishino, A.; Sato, N.; Tsukamoto, Y.; Ueda, K.; Itoh, T.; Sugiyama, Y. Which Concentration of the Inhibitor Should Be Used to Predict in Vivo Drug Interactions From in Vitro Data? *AAPS PharmSci* **2002**, *4* (4), 53−60.

DOI: 10.1021/acs.jmedchem.6b01317
J. Med. Chem. 2017, 60, 2685−2696